


## Fractional Excitations in Non-Euclidean Elastic Plates

Kai Sun and Xiaoming Mao 

Department of Physics, University of Michigan, Ann Arbor, Michigan 48109-1040, USA

 (Received 11 January 2021; accepted 3 August 2021; published 27 August 2021)

We show that minimal-surface non-Euclidean elastic plates share the same low-energy effective theory as Haldane's dimerized quantum spin chain. As a result, such elastic plates support fractional excitations, which take the form of charge-1/2 solitons between degenerate states of the plate, in strong analogy to their quantum counterpart. These fractional excitations exhibit properties similar to fractional excitations in quantum fractional topological states and in Haldane's dimerized quantum spin chain, including deconfinement and braiding, as well as unique new features such as holographic properties and diodelike nonlinear response, demonstrating great potentials for applications as mechanical metamaterials.

DOI: [10.1103/PhysRevLett.127.098001](https://doi.org/10.1103/PhysRevLett.127.098001)

*Introduction.*—The analogy between quantum and classical physics plays an important role in the history of many-body physics. For example, in the early development of quantum topological states, concepts of classical topological defects (e.g., vortices and solitons) have been crucial to the understanding of fractional excitations in fractional quantum Hall systems [1] and quantum spin chains [2,3]. A more recent example is the duality between topological defects in elasticity and fractons in tensor gauge theories [4]. Conversely, quantum topological states of matter inspired the blossoming new field of topological mechanics [5–19]. So far, mechanical analogs have only been achieved for integer quantum topological states, but not yet the more exotic fractional ones.

In a typical quantum system, excitations are usually composed of integer numbers of fundamental building blocks (quanta). However, in certain strongly correlated fractional topological systems, such as fractional quantum Hall systems [20] or  $Z_2$  spin liquids [21], a low-energy excitation is a fraction of the fundamental building blocks, and this phenomenon is known as fractionalization. More specifically, the definition of fractional excitations involves five criteria. (1) “Integer” excitations need to be defined, i.e., the system needs to obey a certain quantization condition, such that excitations can be classified by a certain integer quantum number (e.g., charge). (2) An integer excitation then “breaks up” into multiple pieces. Most importantly, the interactions between these pieces need to decay with their separation in space, known as “deconfinement.” In quantum systems, deconfinement is a highly nontrivial requirement, because it is usually impossible to break a quantum particle, e.g., an electron. In classical physics, it is often possible to partition an object. However, such partition in classical physics usually cannot meet the next criterion. (3) Equal partition has to be enforced as we split the integer excitation. For example, if a charge-1 integer excitation splits into two equal parts,

each part is a fractional excitation with a charge of 1/2. Such equal partition is natural in quantum systems, but a nontrivial requirement in classical systems. Furthermore, two more criteria need to be enforced to ensure that these fractional excitations cannot be trivially mapped back to integer ones: (4) a fractional excitation must be a topological object, which cannot be created by any local deformations, and (5) these fractional excitations must exhibit novel properties impossible for any integer ones, such as braiding [22].

In this Letter, we show that minimal-surface elastic plates support fractional low-energy excitations. Because of the presence of the minimal-surface associate family, these systems exhibit two types of soliton configurations: integer and half-integer, in strong analogy to the quantum integer and fractional excitations in the one-dimensional (1D) dimerized spin chains of Haldane [2]. Following the notion in Refs. [2,3], the term soliton here refers to topological solitons (kinks), instead of solitons arising from nonlinear wave equations. We demonstrate that the classical system and the quantum spin chain share the same low-energy effective theory (compact sine-Gordon), and in both systems, fractionalization is induced by a  $Z_2$  symmetry. As a result, this classical version of fractional excitations shares identical physical properties as their quantum counterpart. For example, integer excitations are conventional and could be created via local deformations, but once it splits into two fractional excitations, each of them is a topological excitation, robust against any local perturbations.

These fractional excitations exhibit exotic mechanical properties, including braiding which is general to fractional excitations, and holographic property and diodelike torque-rotation response which are unique to these minimal-surface plates. These novel properties may find broad applications as mechanical metamaterials.

*2D non-Euclidean plates.*—Non-Euclidean plates are elastic plates having no stress-free configurations.

Their elastic energy is composed of two parts  $E = E_s + E_b$  for stretching ( $E_s$ ) and bending ( $E_b$ ) energies [23,24]. The stretching energy depends on the first fundamental form (i.e., the metric tensor)  $g$  of the manifold

$$E_s = h \int dA \left\{ \frac{B_0 - G_0}{2} \text{tr}(g - g_0)^2 + G_0 \text{tr}[(g - g_0)^2] \right\}, \quad (1)$$

where  $h$  is the thickness of the sheet and the elastic moduli are  $B_0 = \{9BG/[4(3B + 4G)]\}$  and  $G_0 = G/4$  with  $B$  and  $G$  being the 3D bulk and shear moduli of the material respectively.  $E_s$  is minimized if  $g = g_0$ . The bending energy depends on the second fundamental form (i.e., the curvature tensor)  $b$ . In this study, we focus on 2D non-Euclidean *plates*, i.e., thin sheets homogeneous along the thickness direction, so the bending energy takes the following form

$$E_b = h^3 \int dA \frac{G}{12} \left[ \frac{8(3B + G)}{3B + 4G} H^2 - 2K \right], \quad (2)$$

where  $H \equiv \text{tr} b$  and  $K \equiv \det b / \det g_0$  are the mean and Gaussian curvatures respectively. Because  $E_s \propto h$  and  $E_b \propto h^3$ ,  $E_s$  is the dominant part in the small thickness limit  $h \rightarrow 0$ .

We highlight one important symmetry of 2D plates: the elastic energy [Eq. (2)] is invariant if the curvature tensor flips sign ( $b \rightarrow -b$ ), which is a  $Z_2$  symmetry. This  $Z_2$  symmetry originates from the fact that the two sides of a plate are equivalent, and thus the transformation  $b \rightarrow -b$  (equivalent to flipping the two sides) is a symmetry operation that preserves the energy. This  $Z_2$  symmetry plays a crucial role for fractional excitations.

*Minimal surfaces and low-energy effective theory.*—Minimal surfaces are 2D surfaces that minimize their area locally, characterized by  $H = 0$ . In this Letter, we focus on 2D plates whose target metric tensor ( $g_0$ ) is that of a minimal surface. In this case, minimization of elastic energy  $E$  in the  $h \rightarrow 0$  limit gives  $g = g_0$  and  $H = 0$  [25]. However, this does not uniquely determine one ground state. Instead, there exist infinitely many minimal surfaces with  $g = g_0$  and  $H = 0$  and all these configurations are degenerate ground states of  $E$  (where the only nonzero term is  $-2K$  which is fully determined by  $g_0$  and thus is a constant) [26]. This set of minimal surfaces, which share the same metric tensor, are called an “associate family,” and it is known that minimal surfaces in an associate family can be labeled by a phase angle  $\varphi$  [27]. As we vary  $\varphi$ , minimal surfaces in this associate family deform smoothly into each other. As  $\varphi$  increases by  $2\pi$ , the surface returns to its original configuration. One such example, helicoid-catenoid associate family, is shown in Fig. 1(a) [28].

In summary, the associate family that a minimal-surface plate belongs to defines a “soft mode” of this plate, where we can deform the plate with zero elastic-energy cost to the

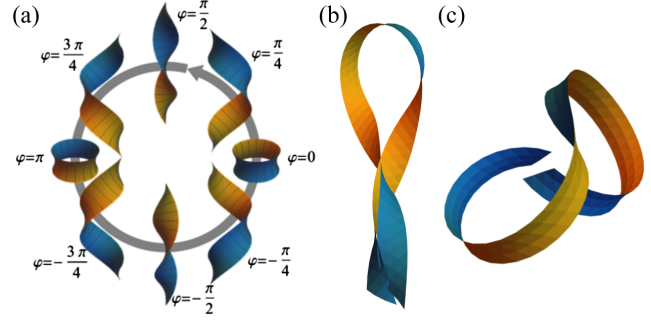


FIG. 1. (a) The helicoid-catenoid associate family. (b),(c) fractional excitation configurations from FEA of ribbons with helicoids (b) and catenoids (c) ground states.

leading order [up to  $O(h^3)$ ]. This soft mode dominates low-energy deformations of such plates.

In particular, we consider a long ribbon of a 2D minimal-surface plate. Here, low-energy excitations can be characterized by a slowly varying  $\varphi$  along the ribbon,  $\varphi(v)$ , where  $v$  is the coordinate along the ribbon. In an ideal minimal-surface plate, because all configurations in the associate family have the same energy, the elastic energy take the following form to the leading order  $E = \int dv [(\partial_v \varphi)^2]$ , i.e., energy cost from inhomogeneity. However, in reality, due to the finite thickness and other deviations from the ideal 2D limit, different configurations in the associate family may have some small energy difference, and thus an additional term arises  $E = \int dv [(\partial_v \varphi)^2 + V(\varphi)]$  [28]. For a generic 2D minimum surface,  $V$  must be a periodic function with  $V(\varphi) = V(\varphi + 2\pi)$  due to the periodic structure of the associate family. For simplicity, here we will take the lowest Fourier harmonic  $V(\varphi) = \gamma \cos(\varphi - \varphi_0)$ , but it must be emphasized that the same qualitative features we discuss below survive even if more complicated  $V(\varphi)$  is considered. As a result, the elastic energy now takes the form of a sine-Gordon theory, which supports soliton solutions. Here, we define the soliton charge as  $\Delta\varphi/(2\pi)$ , where  $\Delta\varphi$  measures the change of  $\varphi$  across a soliton. Because of the periodicity  $V(\varphi) = V(\varphi + 2\pi)$ , it is easy to verify that the soliton solution for this sine-Gordon elastic energy has  $\Delta\varphi = 2\pi$  and thus the soliton charge is one. Therefore, they will be called integer excitations (i.e., integer solitons). This quantization is due to the periodic structure of the associate family.

*Fractional excitations.*—In 2D plates, the  $Z_2$  symmetry discussed above enforces a nontrivial constraint. In a minimal-surface associate family, this  $Z_2$  transformation ( $b \rightarrow -b$ ) corresponds to  $\varphi \rightarrow \varphi + \pi$  in the Weierstrass-Enneper parametrization [27,28]. Thus, it implies that the elastic energy remains invariant under  $\varphi \rightarrow \varphi + \pi$ . We then must also have  $V(\varphi) = V(\varphi + \pi)$ , i.e., the periodicity of the function  $V(\varphi)$  is reduced from  $2\pi$  to  $\pi$ . The elastic energy to the lowest harmonic in  $V(\varphi)$  is then

$$E = \int dv \{ (\partial_v \varphi)^2 + \gamma \cos [2(\varphi - \varphi_0)] \} \quad (3)$$

where an extra factor of 2 arises in the cos function, and thus the soliton of this sine-Gordon theory has  $\Delta\varphi = \pi$ , leading to soliton charge  $1/2$ . These charge- $1/2$  solitons are the fractional excitations.

This mechanism of symmetry-induced fractionalization is identical to the fractional excitations in Haldane’s dimerized spin chain, where fractional spin- $1/2$  solitons arise from a  $Z_2$  symmetry (i.e., translation by an odd integer times the lattice constant) [2]. This physics is also in strong analogy to nematic liquid crystals, where the molecules (and the order parameter) are invariant under a  $\pi$  rotation, and this  $Z_2$  symmetry results in fractional topological defects in nematic liquid crystals, i.e., disclinations or disclination lines, which can be viewed as half of a vortex or a vortex line [29,30].

Guided by the low-energy effective theory, we perform finite element analysis (FEA) of helicoid- and catenoid-ribbons as an example to verify the existence of fractional excitations as their low-energy excitations. In particular, we simulate a narrow ribbon with  $E = E_s + E_b$  as given in Eqs. (1) and (2) with  $g_0$  of the helicoid-catenoid associate family. A small perturbation is added to  $E_b$  to lift the infinite degeneracy of the ground states, favoring either the helicoid ( $\varphi = \pm\pi/2$ ) as ground states or the catenoid ( $\varphi = 0, \pi$ ) as ground states, corresponding to  $\varphi_0 = 0$  and  $\varphi_0 = \pi/2$  in Eq. (3) respectively [28]. This simulation did not enforce the excluded-volume condition, and thus the ribbon may intersect with itself. Enforcing excluded volume doesn’t change any qualitative conclusions.

From the FEA, we found that a fractional excitation is indeed a local energy minimum [Figs. 1(b) and 1(c)]. When the helicoid is the ground state, the fractional excitation is the domain boundary between a left-handed ( $L$ ) section of helicoid and a right-handed ( $R$ ) one. When the catenoid is the ground state, the fractional excitation is also a domain boundary, across which the two sides (inside and outside) of the catenoid flip. The fact that a  $1/2$  excitation corresponds to a domain boundary is universal for any  $1/2$  excitation in any minimal-surface plates, as well as in dimerized quantum spin chains [2]. Because it is a domain boundary, such fractional excitations cannot be created by any local deformations, in contrast to integer excitations, which can be created or removed locally.

In particular, for the helicoid ground states, by minimizing the elastic energy, we find that such a domain structure always bends the ribbon by nearly  $180^\circ$ , i.e., each  $1/2$  excitation implies a sharp U turn. The origin of this sharp turn is that  $\varphi$  changes between  $\pm\pi/2$  across the soliton, thus the soliton profile is characterized by a narrow section of a catenoid, which turns the ribbon.

*Quantum-classical analogy and braiding.*—To set the stage for comparing these classical fractional excitations with their quantum counterparts, we first provide a brief review of 1D dimerized spin chains and 2D  $Z_2$  spin liquids. A 2D  $Z_2$  spin liquid is one of the most important fractional

topological states (see, e.g., Refs. [21,31] and references therein). The study of  $Z_2$  spin liquids originates from Anderson’s resonating-valence-bond (RVB) scenario [32,33] in frustrated quantum spin systems and quantum dimer models [34–36]. This exotic quantum phase of matter is characterized by a topological Ising gauge theory and gives rise to deconfined fractional excitations, e.g., spinons which carry spin- $1/2$  but no charge [37–41]. Later, an exactly solvable model with the same topological order was introduced, known as the toric code model of Kitaev [42]. A 1D dimerized spin chain (e.g., the Majumdar-Ghosh model [43]) does not show a  $Z_2$  topological order, but it shares a certain similar feature as the  $Z_2$  spin liquids.

Here we start from the 1D case by considering the 1D Majumdar-Ghosh model (spin- $1/2$  Heisenberg spins with frustrated nearest and next-nearest-neighbor antiferromagnetic couplings) [43]. This model has two dimerized ground states [Figs. 2(a) and 2(b)], where each box represents a spin singlet pair (a “dimer”). One obvious excitation is to break a dimer, transferring a singlet into a triplet, carrying integer spin  $S = 1$ . The low-energy effective theory of this chain is a sine-Gordon theory (known as Abelian bosonization [44–46]) same as for the ribbon we discuss, where the spin-1 local excitation is a quantum soliton, which can fractionalize into two deconfined spin- $1/2$  solitons [2] [Figs. 2(c) and 2(d)]. In both the quantum model and the ribbon, integer excitations can be created-removed locally (although this is beyond the low-energy theory), but the spin- $1/2$  excitations cannot.

One important and unique property of these fractional particles is that by moving such fractional particles around noncontractible loops, the global state of the entire system can be transformed in a nontrivial way. One such example is “braiding” (i.e., moving particles around each other), which plays a crucial role in the understanding of fractional quantum Hall effects, Majorana modes and topological quantum computing [22]. In 1D, because one cannot move one particle around another as in 2D, a different

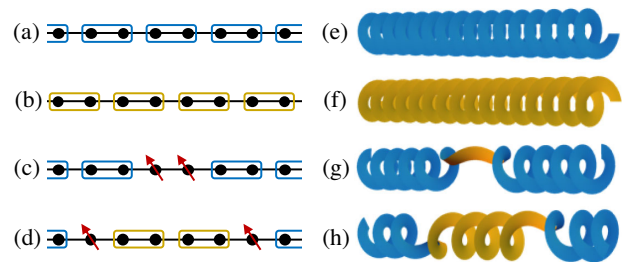


FIG. 2. Analogous fractional excitations in (a)–(d) a dimerized spin chain and (e)–(h) a helicoid ribbon. The spin chain has two degenerate ground states (a) and (b). A spin-1 excitation can be created via local perturbations (c), which splits into two deconfined spin- $1/2$  excitations (d). (e)–(f) The two degenerate ground states with opposite chirality of a helicoid ribbon. (g) A charge-1 soliton can be created locally, and split into two charge- $1/2$  solitons (h).

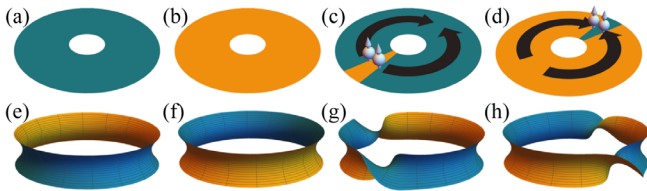


FIG. 3. Fractional excitations and topological degeneracy. (a)–(d) A quantum  $Z_2$  spin liquid on an annulus, with two degenerate ground states (a),(b) due to topological degeneracy. (c) A spin-1 excitation is introduced via local perturbations and split into two spin-1/2 fractional excitations. (d) If these two fractional excitations move around the annulus and annihilated with each other, the system turns from ground state (a) to (b). (e)–(h) A catenoid with the same geometry shows the same property. The two degenerate ground states correspond to swap the two sides of the 2D manifold (e),(f). One can create two charge-1/2 solitons (g) and move them around the catenoid (h), flipping the catenoid to ground state (f).

noncontractible loop is utilized [47] as discussed below, which reflects the same nontrivial impact of a fractional excitations. As shown in Fig. 2(d), moving the two fractional excitations in the 1D Majumdar-Ghosh model away from each other flips the ground state from (a) to (b). This phenomenon also arises in minimal-surface plates [Figs. 2(e)–2(h)]. An integer soliton of charge-1 can be locally generated, and split into two charge 1/2 solitons. This pair of fractional excitations are deconfined, as the ribbon between them is in ground state. Moving this pair of fractional excitations away from each other flips the ribbon between  $R$  and  $L$  helicoids.

For a 2D  $Z_2$  liquid, a similar phenomenon arises [31], where moving a pair of fractional excitation around an annulus flips the topologically degenerate ground states [Fig. 3]. This is analogous to the motion of fractional excitations in the catenoid.

*Holographic property.*—In addition to the analogy to their quantum counterparts, fractional excitations in a helical ribbon have certain unique features. One example is that these solitons are *holographic*, which means that if there is only one charge-1/2 soliton in a helicoid, we can control its location at the two ends of the helicoid. This is because this soliton is the domain boundary between the  $L$  and  $R$  sections. For a helicoid of total length  $l$  and  $L$  section length  $x$ , the helicity of the whole ribbon (i.e., the net number of  $R$  twist) is  $(l - 2x)/\lambda$  where  $\lambda$  is the pitch of the helicoid. This directly relates helicity to the position of the soliton. Thus, by twisting the two ends of the ribbon relative to one another, one can change helicity and the position of the soliton holographically. This holographic control is not a general property of fractional excitations, but a special feature for fractional excitations in helicoids, and provides a natural way to generate these fractional excitations.

*Diodelike torque-rotation response.*—The holographic property of this fractional excitations gives rise to unusual

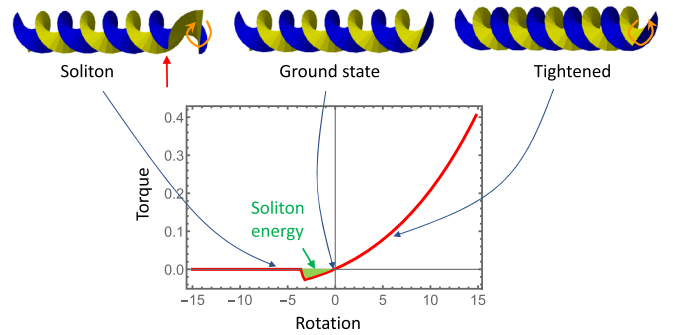


FIG. 4. Diodelike torque-rotation response. Three representative configurations are shown for the ground state (middle), a state with counterclockwise rotation (orange arrow) where the helicoid is tightened (right), and a state with clockwise rotation where a soliton (red arrow) is generated (left).

mechanical response. One prominent example is that when one end of the ribbon is fixed and the center-line of the ribbon is confined to be straight (e.g., by embedding a stiff rod), the torque-rotation relation at the opposite end strongly resembles the current-voltage (IV) characteristics of a diode. We simulated this effect assuming an elastic energy of the form in Eq. (3), and the results are shown in Fig. 4. When counterclockwise rotation is applied to the end of an  $R$  helicoidal ribbon, it tightens the ribbon and leads to a linear torque-rotation response. In contrast, when clockwise rotation is applied to the end of this ribbon, it generates a fractional excitation, which turns the  $R$  helicoid into an  $L$  helicoid. At small counterclockwise rotation the response is still linear (which homogeneously loosens the helicoid), but as the rotation increases, a small barrier (green area in Fig. 4, the energy of one soliton) is overcome and the torque vanishes, as further rotation just moves the soliton to the left, where the elastic energy stays constant. This strong asymmetry resembles the IV characteristics of a diode, where voltage of different directions generates currents of dramatically different amplitudes.

Furthermore, this system exhibits convenient programmability by placing the soliton at different locations in the ribbon which shifts the torque-rotation curve. This effect can potentially be applied to a broad range of problems such as wave rectification, impact mitigation, mode conversion, and mechanical logic circuits.

*Conclusion and discussion.*—We demonstrate that due to minimal-surface associate families, non-Euclidean elastic plates can support low-energy fractional excitations that strongly resemble fractional quantum excitations. These fractional excitations are highly robust and cannot be locally created or destroyed. They exhibit novel mechanical properties such as holographic control and diodelike torque-rotation response. It is worth pointing out that fractional excitations in quantum topological states of matter and discussed here are distinct from fractional solitons in Refs. [48–51], the physics of which is completely different despite the similarity in terminology.

The non-Euclidean plates discussed in this Letter can be realized experimentally through various techniques of metric control, such as stimuli responsive gels, strain engineering, halftone and gray-scale 3D printing [24,52–54]. The unavoidable finite thickness of the ribbon in experiments can be utilized to enforce the  $Z_2$  symmetry of the problem and select different ground states, as the degeneracy of other  $\varphi$  states will be lifted by higher order terms in  $h$ . The unique holographic control and diodelike nonlinear elastic response may open the door to novel mechanical metamaterials. Furthermore, this elastic realization also offers a new system for future explorations for other species of solitons, such as static and traveling breathers, the quantum versions of which has been studied recently [55–59].

In addition, the fractional excitation in the case of helicoid elastic ribbons share a lot of similarities with various types of kinks and perversions between domains of different handedness in other helical structures such as tendrils on climbing plants [60], intrinsically curved rods [61], self-assembled Janus particle spirals [62], elastic bi-strips [63], helical strings [64], and minimal-surface liquid films [65]. These fractional excitations also share similarities with solitons and other localized excitations in elastic sheets [66–69] and out-of-equilibrium 1D models [70,71]. Here we reveal their unexpected link with fractional quantum excitations.

This work is supported in part by National Science Foundation (NSF-EFRI-1741618) and the Office of Naval Research (MURI N00014-20-1-2479).

- 
- [1] R. B. Laughlin, *Phys. Rev. Lett.* **50**, 1395 (1983).  
 [2] F. D. M. Haldane, *Phys. Rev. B* **25**, 4925 (1982).  
 [3] F. D. M. Haldane, *Phys. Rev. Lett.* **50**, 1153 (1983).  
 [4] M. Pretko and L. Radzihovsky, *Phys. Rev. Lett.* **120**, 195301 (2018).  
 [5] C. L. Kane and T. C. Lubensky, *Nat. Phys.* **10**, 39 (2014).  
 [6] E. Prodan and C. Prodan, *Phys. Rev. Lett.* **103**, 248101 (2009).  
 [7] L. M. Nash, D. Kleckner, A. Read, V. Vitelli, A. M. Turner, and W. T. Irvine, *Proc. Natl. Acad. Sci. U.S.A.* **112**, 14495 (2015).  
 [8] P. Wang, L. Lu, and K. Bertoldi, *Phys. Rev. Lett.* **115**, 104302 (2015).  
 [9] R. Süsstrunk and S. D. Huber, *Science* **349**, 47 (2015).  
 [10] J. Paulose, B. G. -g. Chen, and V. Vitelli, *Nat. Phys.* **11**, 153 (2015).  
 [11] J. Paulose, A. S. Meeussen, and V. Vitelli, *Proc. Natl. Acad. Sci. U.S.A.* **112**, 7639 (2015).  
 [12] D. Z. Rocklin, Bryan Gin-ge Chen, M. Falk, V. Vitelli, and T. C. Lubensky, *Phys. Rev. Lett.* **116**, 135503 (2016).  
 [13] D. Z. Rocklin, S. Zhou, K. Sun, and X. Mao, *Nat. Commun.* **8**, 14201 (2017).  
 [14] D. Zhou, L. Zhang, and X. Mao, *Phys. Rev. Lett.* **120**, 068003 (2018).  
 [15] D. Zhou, L. Zhang, and X. Mao, *Phys. Rev. X* **9**, 021054 (2019).  
 [16] L. Zhang and X. Mao, *New J. Phys.* **20**, 063034 (2018).  
 [17] T. C. Lubensky, C. Kane, X. Mao, A. Souslov, and K. Sun, *Rep. Prog. Phys.* **78**, 073901 (2015).  
 [18] X. Mao and T. C. Lubensky, *Annu. Rev. Condens. Matter Phys.* **9**, 413 (2018).  
 [19] K. Sun and X. Mao, *Phys. Rev. Lett.* **124**, 207601 (2020).  
 [20] H. L. Stormer, D. C. Tsui, and A. C. Gossard, *Rev. Mod. Phys.* **71**, S298 (1999).  
 [21] X.-G. Wen, *Rev. Mod. Phys.* **89**, 041004 (2017).  
 [22] C. Nayak, S. H. Simon, A. Stern, M. Freedman, and S. Das Sarma, *Rev. Mod. Phys.* **80**, 1083 (2008).  
 [23] E. Efrati, E. Sharon, and R. Kupferman, *J. Mech. Phys. Solids* **57**, 762 (2009).  
 [24] E. Sharon and E. Efrati, *Soft Matter* **6**, 5693 (2010).  
 [25] E. Efrati, E. Sharon, and R. Kupferman, *Phys. Rev. E* **83**, 046602 (2011).  
 [26] I. Levin and E. Sharon, *Phys. Rev. Lett.* **116**, 035502 (2016).  
 [27] *Handbook of Differential Geometry*, edited by F. J. Dillen and Verstraelen, Vol. 1 (Elsevier, New York, 2000).  
 [28] See Supplemental Material at <http://link.aps.org/supplemental/10.1103/PhysRevLett.127.098001> for a review of minimal-surface associate families, higher order terms and computational modeling of fractional excitations in helicoids.  
 [29] P.-G. De Gennes and J. Prost, *The Physics of Liquid Crystals* (Oxford University Press, New York, 1993).  
 [30] T. C. Lubensky and P. Chaikin, *Principles of Condensed Matter Physics* (Cambridge University Press, Cambridge, England, 2000).  
 [31] E. Fradkin, *Field Theories of Condensed Matter Physics* (Cambridge University Press, Cambridge, England, 2013).  
 [32] P. Anderson, *Mater. Res. Bull.* **8**, 153 (1973).  
 [33] P. Fazekas and P. W. Anderson, *Philos. Mag.* **30**, 423 (1974).  
 [34] S. A. Kivelson, D. S. Rokhsar, and J. P. Sethna, *Phys. Rev. B* **35**, 8865 (1987).  
 [35] D. S. Rokhsar and S. A. Kivelson, *Phys. Rev. Lett.* **61**, 2376 (1988).  
 [36] R. Moessner and S. L. Sondhi, *Phys. Rev. Lett.* **86**, 1881 (2001).  
 [37] N. Read and S. Sachdev, *Phys. Rev. Lett.* **66**, 1773 (1991).  
 [38] X. G. Wen, *Phys. Rev. B* **44**, 2664 (1991).  
 [39] C. Mudry and E. Fradkin, *Phys. Rev. B* **49**, 5200 (1994).  
 [40] T. Senthil and M. P. A. Fisher, *Phys. Rev. B* **62**, 7850 (2000).  
 [41] R. Moessner, S. L. Sondhi, and E. Fradkin, *Phys. Rev. B* **65**, 024504 (2001).  
 [42] A. Kitaev, *Ann. Phys. (Amsterdam)* **303**, 2 (2003).  
 [43] C. K. Majumdar and D. K. Ghosh, *J. Math. Phys. (N.Y.)* **10**, 1399 (1969).  
 [44] P. Francesco, P. Mathieu, and D. Sénéchal, *Conformal Field Theory* (Springer Science & Business Media, New York, 2012).  
 [45] I. Affleck, *Fields, Strings, and Critical Phenomena, USMG, NATO ASI, Les Houches, session XLIX, 1988. Course 10 (Abeline and Non-Abeline Bosonization)* (1988).  
 [46] R. Shankar, in *Low-Dimensional Quantum Field Theories for Condensed Matter Physicists* (World Scientific, Singapore, 1995), pp. 353–387.  
 [47] M. Oshikawa, Y. B. Kim, K. Shtengel, C. Nayak, and S. Tewari, *Ann. Phys. (Amsterdam)* **322**, 1477 (2007).

- [48] B. Collie and D. Tong, *J. High Energy Phys.* **08** (2009) 006.
- [49] M. Nitta and W. Vinci, *J. Phys. A* **45**, 175401 (2012).
- [50] A. Samoilenka and Y. Shnir, *J. High Energy Phys.* **09** (2017) 029.
- [51] A. Samoilenka and Y. Shnir, *Phys. Rev. D* **97**, 045004 (2018).
- [52] A. S. Gladman, E. A. Matsumoto, R. G. Nuzzo, L. Mahadevan, and J. A. Lewis, *Nat. Mater.* **15**, 413 (2016).
- [53] Z. Chen, Q. Guo, C. Majidi, W. Chen, D. J. Srolovitz, and M. P. Haataja, *Phys. Rev. Lett.* **109**, 114302 (2012).
- [54] J. Kim, J. A. Hanna, M. Byun, C. D. Santangelo, and R. C. Hayward, *Science* **335**, 1201 (2012).
- [55] M. Shifman, A. Vainshtein, and J. Wheeler, *From Fields to Strings: Circumnavigating Theoretical Physics* (World Scientific, Singapore, 2005), <https://www.worldscientific.com/doi/abs/10.1142/5621>.
- [56] H. J. Schulz, *Phys. Rev. Lett.* **77**, 2790 (1996).
- [57] F. H. L. Essler, A. M. Tselik, and G. Delfino, *Phys. Rev. B* **56**, 11001 (1997).
- [58] A. W. Sandvik, *Phys. Rev. Lett.* **83**, 3069 (1999).
- [59] C. Zhou, Z. Yan, H.-Q. Wu, K. Sun, O. A. Starykh, and Z. Y. Meng, *Phys. Rev. Lett.* **126**, 227201 (2021).
- [60] A. Goriely and M. Tabor, *Phys. Rev. Lett.* **80**, 1564 (1998).
- [61] G. Domokos and T. J. Healey, *Int. J. Bifurcation Chaos Appl. Sci. Eng.* **15**, 871 (2005).
- [62] Q. Chen, J. K. Whitmer, S. Jiang, S. C. Bae, E. Luijten, and S. Granick, *Science* **331**, 199 (2011).
- [63] J. Liu, J. Huang, T. Su, K. Bertoldi, and D. R. Clarke, *PLoS One* **9**, e93183 (2014).
- [64] C. Nisoli and A. V. Balatsky, *Phys. Rev. E* **91**, 062601 (2015).
- [65] T. Machon, G. P. Alexander, R. E. Goldstein, and A. I. Pesci, *Phys. Rev. Lett.* **117**, 017801 (2016).
- [66] R. D. Yamaletdinov, V. A. Slipko, and Y. V. Pershin, *Phys. Rev. B* **96**, 094306 (2017).
- [67] G. Cao and X. Chen, *Phys. Rev. B* **73**, 155435 (2006).
- [68] H. Diamant and T. A. Witten, *Phys. Rev. Lett.* **107**, 164302 (2011).
- [69] T. G. Sano and H. Wada, *Phys. Rev. Lett.* **122**, 114301 (2019).
- [70] Y. S. Kivshar, N. Gronbeck-Jensen, and M. R. Samuelsen, *Phys. Rev. B* **45**, 7789 (1992).
- [71] K. Alfaro-Bittner, M. Clerc, M. García-Ñustes, and R. Rojas, *Europhys. Lett.* **119**, 40003 (2017).